SIGNATURE ANALYSIS OF DESTROYED BUILDINGS IN SIMULATED HIGH RESOLUTION SAR DATA

Silvia Kuny, Karsten Schulz, Horst Hammer

Fraunhofer Institute of Optronics, System Technologies and Image Exploitation (IOSB), Gutleuthausstr. 1, 76275 Ettlingen, Germany

ABSTRACT

Approaches for urban damage assessment often rely on pre-post-event comparison. In this process the knowledge about damage type specific signature characteristics could be of considerable assistance. This paper presents a signature analysis of the most common damage types of buildings based on simulated high resolution SAR images. A comparison is made between the signature of each damage type and the signature of the corresponding intact building with the purpose of identifying type-specific characteristics, later to be used for a building-wise damage type classification.

Index Terms— SAR simulation, damage assessment, building damage types, characteristic signature

1. INTRODUCTION

When natural disasters such as earthquakes or floods occur in populated areas, time is the most crucial factor for emergency response. Hence methods for damage detection based on remote sensing data are an issue of great interest. SAR imagery offers a substantial advantage over optical imagery, since SAR sensors are not dependent on illumination by the sun or weather conditions, and therefore are particularly suitable for this problem. As damage detection in SAR imagery is an open research issue and widely debated, to date various approaches have been introduced to obtain damage information from SAR data. The most restricting issue for approaches using pre- and post-event images, such as in [1] is posed by the lack of a high resolution pre-event SAR image, since this mode can only be used for specific areas of interest as for example in emergency cases and thus provides no area-wide coverage. For this reason many approaches replace the pre-event SAR image with other imagery or ancillary information [2,3]. Our motivation, however, is the concept of eventually replacing the pre-event image with a SAR simulation of the corresponding area and in doing so having the benefit of working with SAR images of exactly the same imaging parameters as well as possessing information about the positioning of individual buildings. With this in mind we aim for a building-wise damage type classification. With this paper we provide a pre-study, covering a methodical analysis of the most common damage types and the corresponding SAR signatures. Our aim is to identify signature characteristics that are representative for each damage type. This can only be performed if an adequately large data set is available. It is all but impossible to acquire a sufficient number of SAR images of a particular object with the needed systematic variations and consistencies in imaging parameters. Instead this study exploits the advantages a realistic SAR simulator offers to generate the needed data set. Based on 3D models of the most common types of building damages, SAR simulations are compiled, imitating a specific SAR sensor (TerraSAR-X HR Spotlight) by setting corresponding imaging parameters. A comparison between SAR signatures of the intact building and different damage types is carried out to assess the characteristics of the respective type. The SAR simulator used for this purpose is the ray tracing based SAR simulation suite CohRaS [4] developed at Fraunhofer IOSB.

2. SYSTEMATIC ANALYSIS

In order to be able to simulate realistic signatures of building damage types special care had to be taken, to use suitable 3D models as well as to administer adequate settings as input for the simulator.

2.1. Models

The list of damage types chosen for this analysis is based on a compilation of the most commonly occurring types of building damages defined in [5]. When modeling these damage types it is of importance, that the 3D models remain generic but at the same time are distinctly distinguishable from one another. Therefore we came to the conclusion that some of the defined types are to be disregarded, due to their obvious inexpedience for this cause. The 3D models of the damage types being used are displayed in Figure 1. Characteristic signatures of standing structures are often at least partly covered by signatures of the heaps of debris surrounding the building. In order to record these characteristic signatures and to create a signature of the respective damage type which is as realistic as possible, each type is modeled

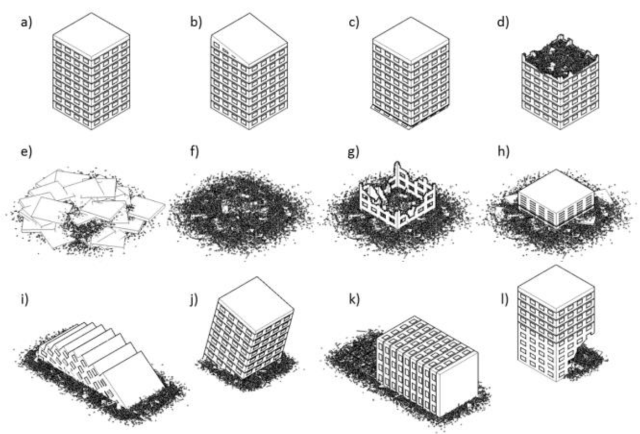

Figure 1: 3D models of common building damage types. a) Intact, b) Inclined plane, c) Pancake collapse (first floor), d) Heap of debris on uncollapsed stories, e) Heap of debris with planes, f) Heap of debris, g) Heap of debris with vertical elements, h) Pancake collapse (all stories), i) Outspread multi-layer collapse, j) Inclination, k) Overturn collapse, l) Overhanging elements.

with a heap of debris and without it. The generation of the heaps of debris was carried out automatically using an algorithm with variable settings for height, size and composition of the heaps.

2.2. Simulation

CohRaS is a SAR simulator based on raytracing that directly simulates processed SAR images (i.e. no raw data are created). Both amplitude and phase of the backscattered signals are simulated, making the coherent processing of different signal contributions possible. It uses efficient raytracing algorithms and features a batch mode that can be used for the creation of whole series of simulated images such as those shown in this paper. More details about CohRaS can be found in [4].

In order to simulate signatures comparable to those of TerraSAR-X images in High Resolution Spotlight mode corresponding sensor and imaging parameters were used, e.g. a wavelength of 3.1 cm and a pixel spacing of 45 cm in range and 87 cm in azimuth. Each model was simulated for a full range of aspect angles from 0° to 359° in steps of 1°, so the dependence of the signatures on this angle can be inspected. Parameters for the material properties were chosen such, that the amplitudes of real signatures showing a comparable intact building are imitated. Even though the simulated amplitudes are not calibrated, and thus cannot be compared directly to real SAR data, a comparison of proportional amplitude differences is valid. It was differentiated between material for building, ground, glass and debris, where glass was provided with very specular properties, and building and ground were modeled to be less specular but with

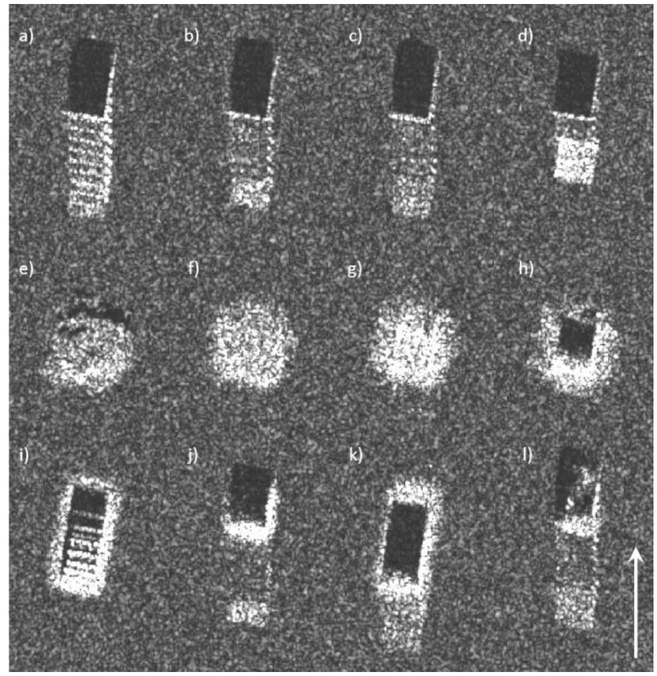

Figure 2: simulated amplitude images corresponding to the 3D models in Fig. 1, including heaps of debris (range direction indicated by arrow).

moderate direct reflectance. Real SAR signatures of an intact comparable building show very strong backscattering from window ledges, due to the formation of dihedral and trihedral corner reflectors with the glass. Since glass is one of the weakest points of a building and thus the first to burst in a destructive event we presumed that any damage type that is addressed in this paper is severe enough to warrant a destruction of all the glass. Due to the fact that removing the glass leads to a great deal of multi-bounces inside the unrealistic empty interior of the building, the glass was instead given a non-reflective material. In Figure 2 the final simulated amplitude images for one aspect angle are displayed.

3. RESULTS

Any maximal or mean values given in the following are obtained from a fixed cutout of the amplitude images that contains the entire building signature including the shadow. The signature of the intact building consists mainly of a dihedral corner, resulting from specular bounce involving the ground and the vertical wall, little direct reflection, shadow and trihedral corner points resulting from the window ledges in combination with the highly specular glass. Since the simulations for all damage types were conducted with a non-reflective material for the glass areas, the same was done for the intact building. A comparison of amplitude images and their maximal values can be seen in Figure 3. The dihedral corner lines turn out to be distinctively weaker without the reflective glass best seen for frontal viewing angles

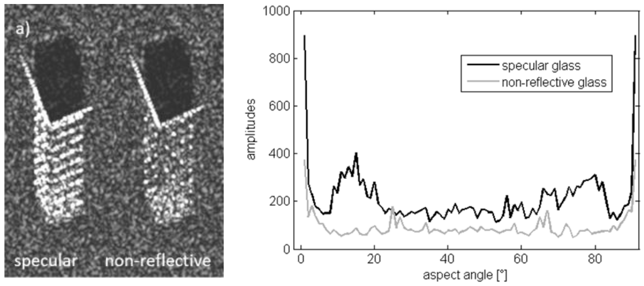

Figure 3: a) simulated amplitude image of intact building with specular (left) and non-reflective (right) material for glass areas, b) maximal values occurring in amplitude images for an aspect angle interval of 90°.

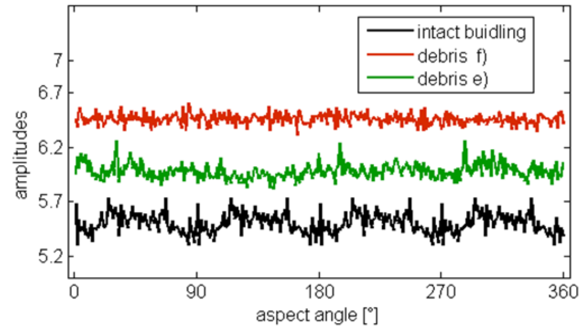

Figure 4: Comparison of mean amplitudes occurring for small rubble (red), debris with planes (green) and intact building (black) for 360 aspect angles.

(e.g. 0°, 90°). The window ledges lead to the strongest trihedral corner reflection for aspect angles between 9° and 22° (68°-81°) in the case of specular glass, for non-reflective glass there are only much weaker dihedral corner signatures. Since the glass-induced strong reflectance is no damage type specific feature, the following comparisons are made regarding the intact building with non-reflecting glass.

The damage types b) and c) are the least severe for this analysis, and accordingly show only little indication of any change. Even so, an inclined plane, as is the case in b), leads to either stronger or weaker direct reflection of the roof depending in which direction the plane is tilted, as well as an insignificantly weaker dihedral corner line. A severe contortion alike the one in c), a sideward shift of the upper stories, yields a distinct shift of the dihedral corner in range direction and at a view perpendicular to that a shift of the entire signature in azimuth direction. However, we presume that these two damage types are more likely to be detected by the signature of surrounding debris than the mentioned changes. Debris occurring in many different shapes is a main source of the signature of damaged buildings and simulations of this were shown in [6]. Its dependence on the macroscopic surface roughness, in the sense of larger planes versus small rubble was investigated in an earlier analysis [7]. In [7] the observation that small rubble tends to cause a visibly stronger signature due to many dihedral and trihedral corner reflectors being formed, while a more planar surface reflects the beam away from the sensor, was confirmed. This can be observed in this case also, comparing the simulation of damage types e) and f) in Figure 2. The mean amplitudes of e) are distinctively smaller than those of f) for all aspect angles, and the undestroyed building has the lowest mean amplitudes of the three (see Figure 4). However, due to the occurrence of large corner reflectors, e) contains higher maximal values. In the case of still standing structures amidst the debris (g), there are characteristic signatures due to the missing roof and hence the view to the interior of the remaining structure. Consequently strong dihedral and trihedral corner signatures occur, causing high backscattered intensity. Surrounding debris reduces these signatures significantly and in return yield higher average amplitudes due to the many small corner reflectors. If debris is piled up high, like in this case, potential corner reflectors are positioned higher as well and thus the signature is shifted in range direction. For debris occurring even higher, on the top of uncollapsed stories (d), the corresponding signature is positioned depending on the new height of the building. To what extend the reduction of the dihedral corner or the smaller shadow due to the height loss are reliable indications is strongly correlated with the height reduction. For damage type h), where all stories have collapsed to a minimum, this is a characteristic trait, as well as the lack of any building signature in the expected space in front of the building. The simulations show that an outspread building collapse (i) yields very characteristic signatures. Depending on the aspect angle regarding the building at hand the signature extends distinctly beyond that of the intact building. It was expected that a model shaped with so many very large dihedral corner reflectors results in very strong backscattered intensities. An inclination of the building (j) has a strong effect on some of the dihedral corners, since at least two of the four walls are not perpendicular to the ground anymore. Thus the double bounce yields weaker intensities, which are then projected not to one line but to an area. Either the tilt is visible via the changed tilted position of the signature or the changed direct reflection of the roof depending on the aspect angle. Overhanging elements (l) cause a partial view to the interior of the building and thus possibly direct reflection inside the otherwise undisturbed shadow area. If viewed frontal to the building edge that is overhanging, even a partial loss of the dihedral corner can be observed.

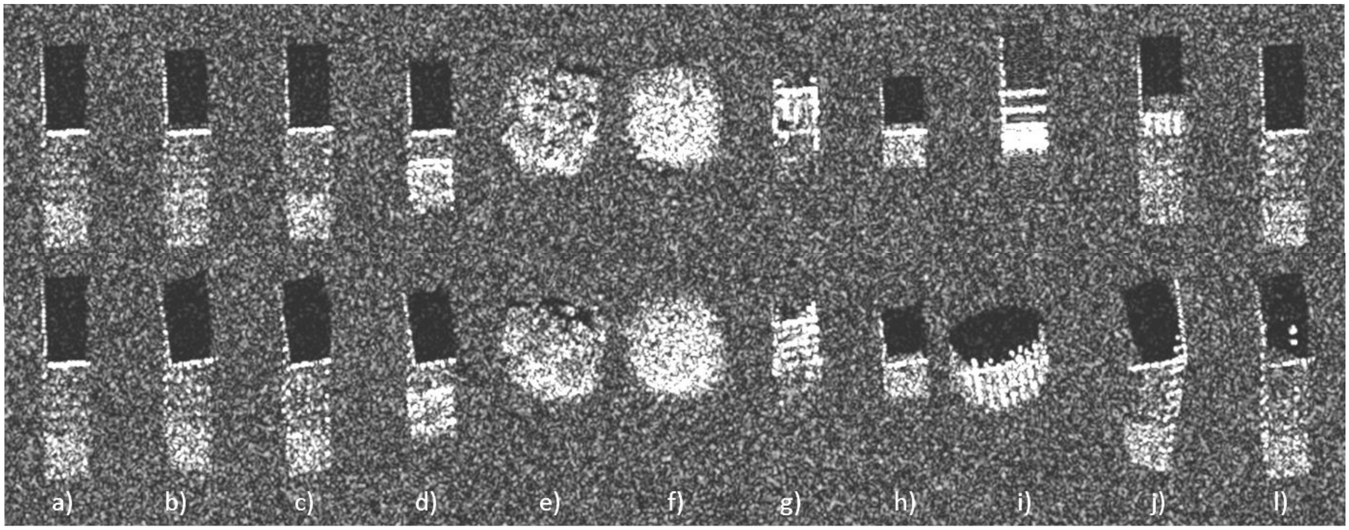

Figure 5: simulated amplitude images corresponding to the 3D models in Fig. 1 without additional heaps of debris for aspect angle 3° (top) and 99° (bottom).

4. CONCLUSION

The SAR signatures of damaged buildings with different types of damage were analyzed using simulated SAR data. The aim of this paper was to identify characteristic changes specific to each damage type in comparison to those of a corresponding intact building as a step towards a reliable categorization of damage types. Even though not all aspect angles provide the same amount of characteristic signatures, we could successfully demonstrate that each damage type features distinctive attributes that are very promising. The observation of higher intensity in the signature of damaged buildings due to rubble could be confirmed as well as the dependence on macroscopic surface roughness.

To which extent it is possible to derive the specific damage type will be matter of a later research. Furthermore we plan to conduct an extensive comparison of the simulated scenes with real SAR data and the corresponding ground truth, so as to confirm their validity.

5. REFERENCES

[1] M. Matsuoka and F. Yamazaki, "Use of satellite SAR intensity imagery for detecting building areas damaged due to earthquakes," in Earthquake Spectra, vol. 20, no. 3, pp. 975-994, August 2004.

[2] F. Dell'Acqua, P. Gamba, and D. Polli, "Mapping earthquake damage in VHR radar images of human settlements: Preliminary results on the 6th April 2009, Italy case," in Proc. of IEEE International Geoscience and Remote Sensing Symposium (IGARSS), Honolulu, HI, USA, pp. 1347-1350, July 2010.

[3] D. Brunner, G. Lemoine, and L.Bruzzone, "Earthquake damage assessment of buildings using VHR optical and SAR imagery," in IEEE Transactions on Geoscience and Remote Sensing, vol. 48, no. 5, pp. 2403-2420, May 2010.

[4] H. Hammer and K. Schulz, "Coherent simulation of SAR images," in Proc. of SPIE, Image and Signal Processing for Remote Sensing XV, Vol. 7477, Berlin, Germany, pp.74771G-1-9, 2009.

[5] C. Schweier and M. Markus, "Assessment of the search and rescue demand for individual buildings," in Proc. of 13th World Conference on Earthquake Engineering, Vancouver, B.C., Canada, Paper No. 3092 , August 2004.

[6] T. Balz and M. S. Liao, "Building-damage detection using post-seismic high-resolution SAR satellite data," International Journal of Remote Sensing, 31 (13) (2010), pp. 3369–3391, 2010.

[7] S. Kuny, K. Schulz and H. Hammer, "Simulation based texture analysis of heaps of debris for damage assessment in high resolution SAR data," to be published in Proceedings of RAST 2013, Istanbul